



## Structure, dielectric, magnetic and magnetoelectric coupling properties of $x\text{PbTiO}_3/(1-x)\text{NiFe}_2\text{O}_4$ composite ceramics

Zhixin Zeng<sup>1,2</sup>, Ruicheng Xu<sup>1,2</sup>, Li Cheng<sup>1,2</sup>, Jinyu Liu<sup>1,2</sup>, Heng Wu<sup>1,2</sup>, Xiaofeng Qin<sup>1,2</sup>, Shulin Xing<sup>1,2</sup>, Xiaoling Deng<sup>1,2,\*</sup>, Rongli Gao<sup>1,2</sup>

<sup>1</sup>School of Metallurgy and Materials Engineering, Chongqing University of Science and Technology, Chongqing 401331, China

<sup>2</sup>Chongqing Key Laboratory of Nano/Micro Composite Material and Device, Chongqing 401331, China

Received 20 February 2020; Received in revised form 26 April 2020; Accepted 13 July 2020

### Abstract

In this paper,  $x\text{PbTiO}_3/(1-x)\text{NiFe}_2\text{O}_4$  (PTO/NFO,  $x = 0.1, 0.2, 0.3, 0.4$  and  $0.5$ ) ceramic composites were prepared by mixing of sol-gel synthesized PTO and NFO powders, followed by their uniaxial pressing and sintering at  $1150^\circ\text{C}$ . The effects of PTO/NFO composition on crystal structure, surface morphology, electrical, magnetic and magnetoelectric coupling properties were studied. XRD results showed that the prepared ceramics contain only PTO and NFO phases without any impurity phase. The samples were relatively dense while the grains were evenly distributed. The dielectric constant and loss varied monotonically with the frequency for different molar ratios. The hysteresis loop of the composites with high amount of high resistance NFO phase ( $x = 0.1, 0.2$ ) has the shape characteristic for a material with large leakage current. The samples with  $x = 0.1$  showed the largest saturated magnetization, while the sample with  $x = 0.2$  had the maximum remnant magnetization. It was also shown that the polarization was affected by the external magnetic field of  $1\text{ mT}$  and the strongest ME coupling (relative polarization change of  $15.4\%$ ) was observed for the  $0.5\text{PbTiO}_3/0.5\text{NiFe}_2\text{O}_4$  composite. In addition, the relevant calculation showed that the leakage mechanism may not be the main factor affecting the polarization of the obtained ceramics.

**Keywords:**  $\text{PbTiO}_3/\text{NiFe}_2\text{O}_4$  ceramics, ferroelectric, ferromagnetic, magnetoelectric coupling effect

### I. Introduction

Multiferroic materials refer to materials with two or more orders of ferroelectric (antiferroelectric), ferromagnetic (antiferromagnetic) and ferroelastic [1–3]. Due to its unique ME coupling properties, multiferroic materials have some special physical properties, some meaningful and new physical phenomena are initiated [2,4]. With the continuous development of information technology, multiferroic materials have a wide range of potential applications in multi-function devices such as transducers, sensors, memories, etc. [5–7].

Multiferroics can be divided into single-phase and composite multiferroic materials [8]. Single-phase multiferroic materials are ferroelectric and ferromagnetic materials under certain conditions [9,10]. The Curie

temperature of most single-phase multiferroic materials is lower than room temperature, limiting their practical applications. A typical room temperature single phase multiferroic material is  $\text{BiFeO}_3$ , which is one of the most studied lead-free multiferroic materials due to its high ferroelectric ( $T_C \sim 1103\text{ K}$ ), antiferromagnetic ( $T_N = 643\text{ K}$ ) transition temperatures and large ferroelectric polarization of  $100\ \mu\text{C}/\text{cm}^2$  in thin films [11–13]. However, the coupling effect of  $\text{BiFeO}_3$  at bulk scale is usually very low mostly due to its poor spontaneous polarization, weak ferromagnetism (antiferromagnetic) and high leakage current density. Therefore, it has been not yet exploited for device application and researchers turned their attention to a new type of multiferroics (composite multiferroic materials).

Composite multiferroic materials take advantage of the ME coupling between two or more single-phase compounds without multiferroic properties, thus, the composite material with a good ME coupling effect is

\*Corresponding author: tel: +86 13508398567, e-mail: [dgxmd@163.com](mailto:dgxmd@163.com)

formed. It was found that the ME coupling coefficient of composite materials was several times higher than that of single-phase materials [14–16]. Composite multiferroic materials are generally composed of ferroelectric and ferromagnetic phase materials. Ferroelectric phase materials are usually selected with good piezoelectric properties and high Curie temperature, while ferromagnetic phase materials are selected with strong magnetostrictive effect.  $\text{PbTiO}_3$  (PTO) is a typical piezoelectric material with high Curie ferroelectric temperature ( $T_C \sim 490^\circ\text{C}$ ). In addition, it has important applications in electronic devices because of its high thermoelectric coefficient ( $250\ \mu\text{C}/\text{cm}^2\ \text{K}$ ) and low dielectric constant [17].  $\text{NiFe}_2\text{O}_4$  (NFO) is an inverse spinel ferrite with high Curie temperature ( $T_C \sim 550^\circ\text{C}$ ) [7]. Meanwhile, NFO is also a typical soft magnetic material with low coercivity, easy magnetization, easy demagnetization, high permeability and resistivity. Therefore, in this study PTO and NFO are selected as the ferroelectric and ferromagnetic phases of composite materials, respectively.

The mixing of ferroelectric phase and ferromagnetic phase with different molar ratios will significantly affect the magnetoelectric properties of composite materials. However, due to the influence of macroscopic mechanical defects, ferromagnetic and ferroelectric phase polymerization, bonding and other factors, the properties of composite materials are deteriorating. In order to resolve this problem,  $x\text{PbTiO}_3/(1-x)\text{NiFe}_2\text{O}_4$  ( $x = 0.1, 0.2, 0.3, 0.4$  and  $0.5$ ) composite ceramics were prepared and the effects of different molar ratios on the properties of the composite ceramics were studied.

## II. Experimental method

The  $x\text{PTO}/(1-x)\text{NFO}$  composite powders were synthesized by sol-gel method.  $\text{Pb}(\text{CH}_3\text{COO})_2 \cdot 3\text{H}_2\text{O}$ , and  $\text{Ti}(\text{C}_4\text{H}_9\text{O})_4$  were dissolved in  $\text{C}_3\text{H}_8\text{O}_2$ , whereas  $\text{Ni}(\text{NO}_3)_2 \cdot 6\text{H}_2\text{O}$  and  $\text{Fe}(\text{NO}_3)_3 \cdot 9\text{H}_2\text{O}$  were dissolved in  $\text{CH}_3\text{CH}_2\text{OH}$  by stirring. After stirring and heating at  $80^\circ\text{C}$  for 1 h, precursor PTO and NFO powders were obtained. The PTO and NFO precursor powders were dried separately and heated at  $900^\circ\text{C}$ . Finally, the PTO and NFO powders were mixed at five different molar ratios to obtain  $x\text{PbTiO}_3/(1-x)\text{NiFe}_2\text{O}_4$  where  $x = 0.1, 0.2, 0.3, 0.4$  and  $0.5$ . The precursor powders were mixed by hand grinding for about 1 h and mixed with PVA (15 wt.%). Pressed pellets with the diameter of 1 cm and the thickness of 0.8 mm were obtained by uniaxial pressing for 10 min at 10 MPa. The PVA was discharged at  $500^\circ\text{C}$ , and the ceramics was finally sintered at  $1150^\circ\text{C}$ .

The X-ray diffraction (SmartLab, Rigaku, Japan) was used to study the crystalline structure using  $\text{Cu}(\text{K}\alpha)$  radiation source ( $\lambda = 1.54178\ \text{\AA}$ ) and  $2\theta$  range from  $20$  to  $80^\circ$ . The surface morphology of the ceramics was investigated by scanning electron microscopy (S-3700N, Hitachi, Japan). The ferroelectric and leakage current

characteristics were determined by ferroelectric test system (TF2000e, aixACCT Inc., Germany). The dielectric permittivity was investigated by using impedance analyser (E4980A, Agilent, USA). The magnetic properties of MPMS SQUID VSM DC magnetometer (Quantum Design, America) were tested at room temperature.

## III. Results and discussion

### 3.1. Structural characterization

The XRD patterns of the PTO/NFO ceramics are shown in Fig. 1. It can be seen that PTO and NFO phases (JCPDS No. 78-0299 and JCPDS No. 74-2081) exist in the composite ceramics. PTO phase has the structure of tetragonal perovskite, with the space group  $P4mm$  and the lattice constant  $a = b = 3.94\ \text{\AA}$ ,  $c = 4.063\ \text{\AA}$ . NFO phase has spinel ferrite structure with the space group  $Fd\bar{3}m$  and the lattice constant  $8.39\ \text{\AA}$ . There were no other impurity phases. The diffraction peak intensities of NFO with crystal plane index of (220), (311) and (400) increase firstly and then decrease with the increase of PTO content (the samples with  $x = 0.4$  and  $0.5$ ), and the intensity of characteristic PTO peaks was relatively high. This may be because the perovskite PTO was doped with a small amount of  $\text{Fe}^{3+}$  ( $0.64\ \text{\AA}$ ) and  $\text{Ni}^{2+}$  ( $0.69\ \text{\AA}$ ) at the  $\text{Ti}^{4+}$  ( $0.68\ \text{\AA}$ ) ion site with the increase of the PTO molar amount. This displacement may change the size of the cell or cause anisotropic local strain, which may lead to changes in the intensity of the diffraction peaks. When the PTO mole amount increases to  $x = 0.4$  and  $0.5$ , the ceramic system becomes stabled and the diffraction peak strength increased [17,18]. At the same time, when the PTO mole amount is increased, the increase of lead ( $\text{Pb}^{2+}$ ) can restore the A ion sited and enhanced the diffraction peaks of the crystal surface [9,19]. On the one hand, the weak diffraction peaks of the 0.3PTO/0.7NFO ceramics may be related to the sintering behaviour or due to the different sintering activities of the ceramic materials with different molar ratios, which can cause differences in grain size, crystallinity, grain distribution uniformity, etc.

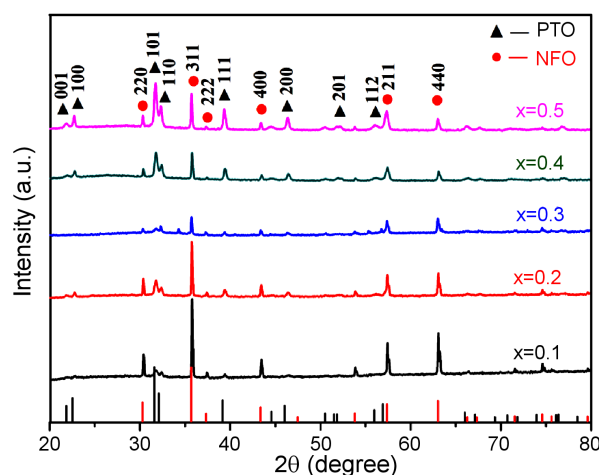


Figure 1. XRD patterns of sintered PTO/NFO ceramics

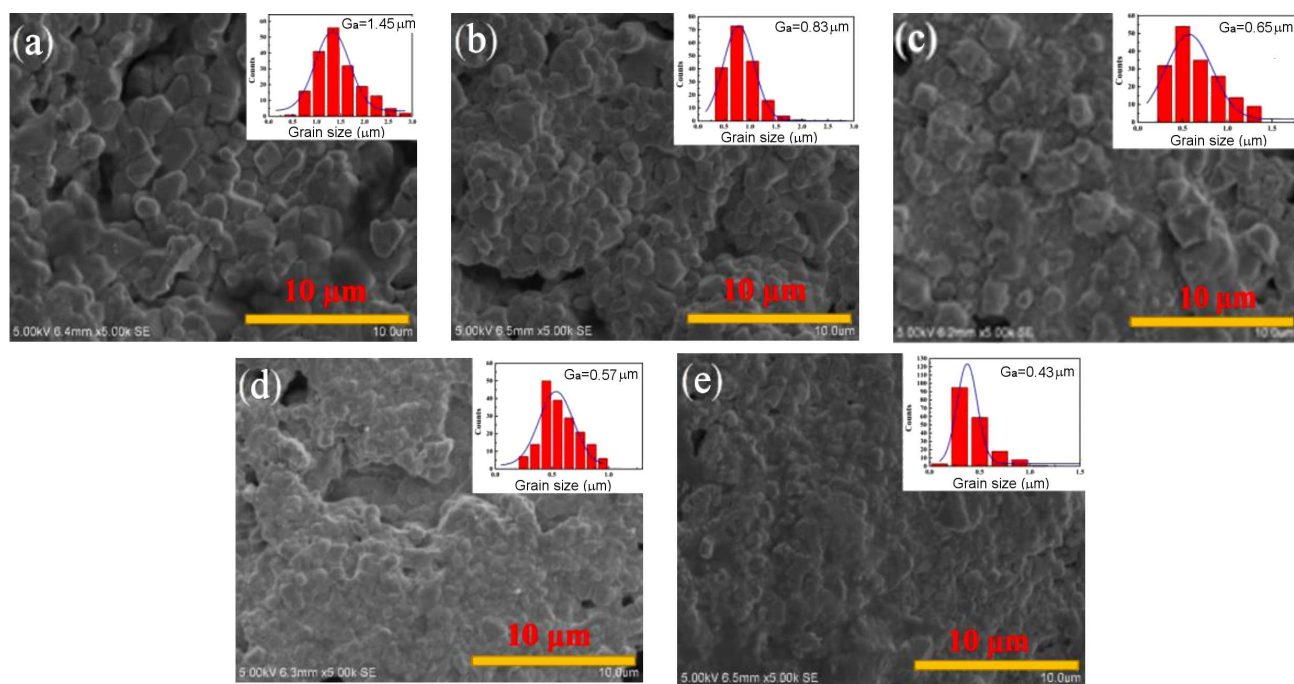


Figure 2. SEM micrographs of  $x\text{PbTiO}_3/(1-x)\text{NiFe}_2\text{O}_4$  ceramics: a)  $x = 0.1$ , b)  $x = 0.2$ , c)  $x = 0.3$ , d)  $x = 0.4$  and e)  $x = 0.5$

Table 1. The porosity and grain size of PTO/NFO composite ceramics

Sample composition	$x = 0.1$	$x = 0.2$	$x = 0.3$	$x = 0.4$	$x = 0.5$
Porosity [%]	11.6	11.1	8.4	11.5	6.8
Grain size [ $\mu\text{m}$ ]	1.45	0.83	0.65	0.57	0.43

The SEM micrographs of the PTO/NFO ceramics are shown in Fig. 2 and the values of porosity and grain size, calculated by the software Nano Measurer, are listed in Table 1. The porosity values for the composites surface with  $x = 0.1, 0.2, 0.3, 0.4, 0.5$  are 11.6, 11.1, 8.4, 11.5 and 6.8%, respectively. Therefore, the relative densities of the inferred material were relatively poor. This may be caused by uneven dispersion of the PTO and NFO phases, agglomeration and linkage of two-phase materials. The observed pores exist due to several reasons. The first of all, it may be that the pressure applied during the preparation of the ceramic sheet is uneven, resulting in poor sample compactness. Secondly, the particle size of powder also affects the formation of stomata. Thirdly, PVA forms carbon dioxide and other gases in the sintering process, forming pores. Finally, during the preparation of magnetolectric composites, more grain boundaries will be generated, and the increase of grain boundaries will lead to the increase porosity. The 0.5PTO/0.5NFO ceramics had relatively flat surfaces and uniform grain distributions, which indicated that the compactness of the ceramics sintered by the two-phase materials with this composition was better than for the other samples.

### 3.2. Dielectric properties

The relationships between the dielectric constant, loss and frequency of the PTO/NFO ceramics are shown in Fig. 3. As the frequency increased, the dielectric constant of all ceramics decreased rapidly in the low-

frequency range and then slightly decreased in the high-frequency region ( $>5$  kHz). Since all relaxation times are much lower than the period of the electric field (in the lower frequency range), all polarization processes can be established to obtain higher dielectric constants. At higher frequencies contributions of ion and orientation polarizability become insignificant, since corresponding electric dipole will not follow the alternating electric field, resulting in a static value of the dielectric constant. The dielectric loss decreased as the frequency increased, because dielectric loss was mainly

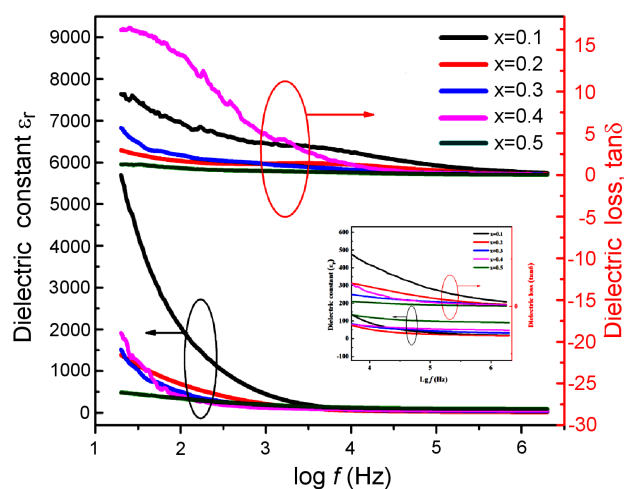


Figure 3. Dielectric constant and loss of PTO/NFO ceramics versus frequency (inset represents high-frequency range)

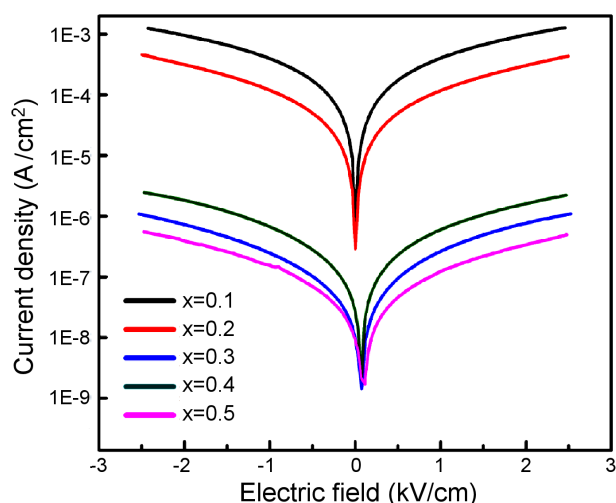


Figure 4. Leakage current of PTO/NFO ceramics

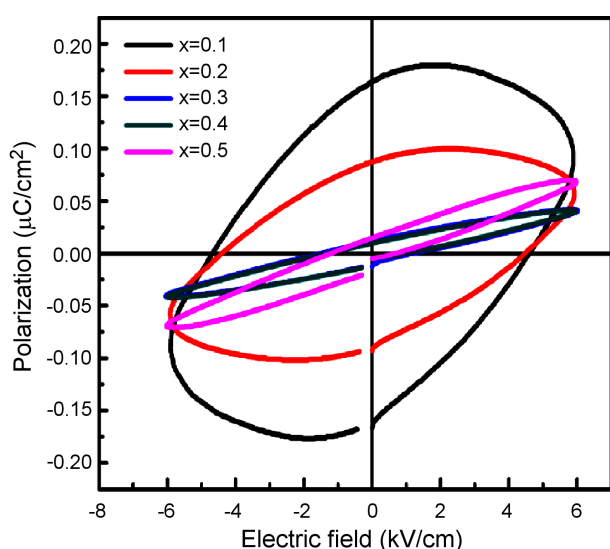


Figure 5.  $P$ - $E$  curves of PTO/NFO ceramics

composed of relaxation loss and conduction loss. Relaxation loss was caused by relaxation polarization, while conduction loss was usually caused by the presence of more or less conductive electrons, holes and some weakly constrained ions in the sample instead of ideal insulators. As mentioned above, the dielectric constant of the sample in the low frequency range was larger, which was mainly caused by relaxation polarization. Therefore, large loss may occur in the low frequency range. With the increased of frequency, dielectric loss decreases obviously, which indicated that the dielectric dispersion follows the Maxwell-Wagner interface polarization [20–22]. At low frequencies, the dielectric loss of the PTO/NFO was very large, which may be due to

the free loss caused by partial discharge of the materials and the conductance loss caused by internal defects and vacancies under the action of external voltage. The dielectric constant of the 0.1PbTiO<sub>3</sub>/0.9NiFe<sub>2</sub>O<sub>4</sub> ceramics was large and with the increase of PTO component the dielectric constant of ceramic decreased. This was because at low frequency, the main contribution to the dielectric constant of ceramics was ferromagnetic material NFO [23–25]. The dielectric loss of the PTO/NFO ceramics was relatively large at low frequency, which may be due to the concentration of defects (such as grain boundary, pores) and other factors. The very large dielectric loss of the 0.1PbTiO<sub>3</sub>/0.9NiFe<sub>2</sub>O<sub>4</sub> ceramics may be due to the large number of pores and roughness on the surface, as can be seen from the SEM of the ceramics in Fig. 2.

The leakage current of the PTO/NFO ceramics is shown in Fig. 4. The leakage current density was found for the composites with  $x = 0.1$  and  $0.2$ , which was because of the high conductivity of NFO phase. It may also be caused by internal defects and lower densities of these ceramics, which led to increased resistance, increased current loss, and thus larger leakage current. In addition, with the increase of external electric field, internal defects began to be amplified, and the carrier generated by defects started to become the most important factor of leakage current.

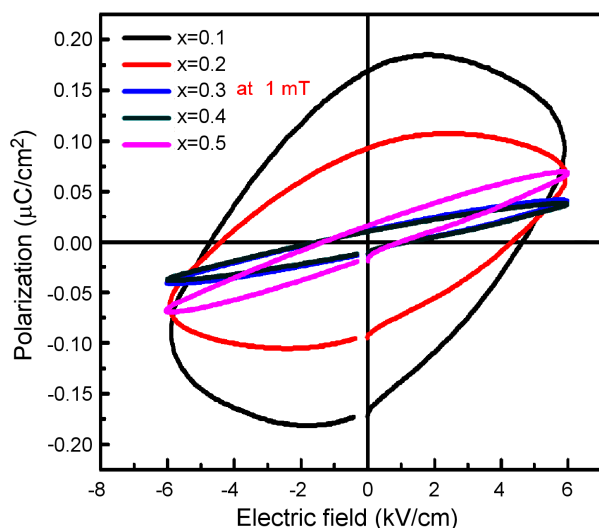
Room temperature  $P$ - $E$  curves of the PTO/NFO ceramics are shown in Fig. 5, and the ferroelectric parameters are also listed in Table 2. The test frequency was 2 kHz. The  $P$ - $E$  curve of the ceramics was selected at high frequency to reduce the effect of leakage current on the ferroelectric hysteresis loop. However, because of the presence of impurities, pores and grain boundaries, the leakage current cannot be ignored and will have a great influence on these measurement results, such as  $P_r$  and  $E_c$  will be overestimated [14]. The behaviour of ferroelectric hysteresis loop was consistent with that of the previously discussed sample leakage current. The results show that the ferroelectric and dielectric properties of ceramics are improved at  $x = 0.5$  due to the suppression of leakage current. As shown in the figure for the ceramic samples when  $x = 0.1$  and  $0.2$ , the  $P_r$  and  $E_c$  of the ceramic exhibit abnormally large values. It was noted that with the increase of PTO molar ratio, the coercive electric field ( $E_c$ ) value decreases (shown in Table 1). On the one hand, the inversion of ferroelectric domain needs to overcome the barrier effect, which increased with the decreased of grain size, the smaller the grain size was, the stronger the coercive force field was. Meanwhile, with the increase of ferroelectric phase grains, ferroelectric domain inversion was easy [26]. On the other hand, the presence of an oxygen vacancy

Table 2. Ferroelectric performances of  $x$ PTO/(1- $x$ )NFO ceramics

Sample composition	$x = 0.1$	$x = 0.2$	$x = 0.3$	$x = 0.4$	$x = 0.5$
$P_r$ [ $\mu\text{C}/\text{cm}^2$ ]	0.164	0.087	0.011	0.009	0.013
$E_c$ [kV/cm]	4.65	4.51	1.22	0.99	0.68

**Table 3.** Residual polarization without magnetic field  $P_r(0)$ , under the magnetic field of 1 mT  $P_r(H)$  and relative change  $[P_r(H) - P_r(0)]/P_r(0)$  of PTO/NFO ceramics

Sample composition	$x = 0.1$	$x = 0.2$	$x = 0.3$	$x = 0.4$	$x = 0.5$
$P_r(0)$ [ $\mu\text{C}/\text{cm}^2$ ]	0.164	0.087	0.011	0.009	0.013
$P_r(H)$ [ $\mu\text{C}/\text{cm}^2$ ]	0.169	0.092	0.0103	0.0096	0.015
Relative change [%]	3	5.7	2.7	6.7	15.4

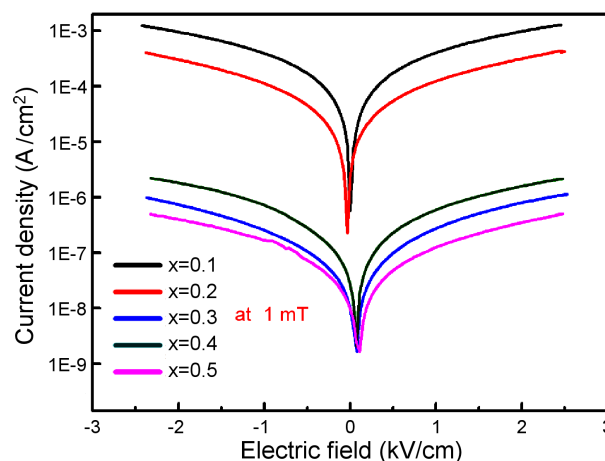
**Figure 6.**  $P$ - $E$  curves of  $x$ PTO/(1- $x$ )NFO ceramic measured under magnetic field of 1 mT

created a barrier, or domain pinning, that prevented domain walls from moving [27].

### 3.3. Magnetoelectric properties

The  $P$ - $E$  curves of the  $x/(1-x)\text{NiFe}_2\text{O}_4$  ceramics under the action of a magnetic field are shown in Fig. 6. Residual polarization ( $P_r$ ) of the PTO/NFO ceramics with and without magnetic field is shown in Table 3. There are only small changes between the ferroelectric hysteresis loop of the PTO/NFO ceramics with and without an external magnetic field, and the shape of the hysteresis loop was basically unchanged. The reason could be relatively small external magnetic field. As shown in Table 3, the residual polarization of the ceramic continuously increases, under the action of a magnetic field, with increase of  $x$ , i.e. PTO content, except for the composite with  $x = 0.3$ . This may be due to the fact that when  $x = 0.3$ , macroscopic defects such as pores, slits of the ceramic caused a decrease in material density, resulting in a tip stress concentration effect, thus let to a series of properties of materials. Under the action of magnetic field, although the  $P$ - $E$  curves were not change much, the change in the residual polarization of the ceramics was relatively obvious, and the residual polarization of ceramics was the largest when  $x = 0.5$ , and the relative change rate was 15.4%, showing a good ME coupling effect. This shows that when the molar ratio of ferroelectric phase and magnetic phase is relatively equal, the magnetoelectric coupling effect may be the highest.

In order to confirm whether the changes in  $P$ - $E$  curves under the action of the external magnetic field were

**Figure 7.** Leakage current of PTO/NFO ceramics exposed to an external magnetic field of 1 mT

caused by the change of the leakage current, the leakage current of the ceramics were measured under the action of the magnetic field (as shown in Fig. 7). Comparing with the leakage current of a ceramic without a magnetic field (Fig. 8), it can be found that the leakage current density of the ceramics slightly changes under the action of the magnetic field. From the leakage current curves in the presence or absence of magnetic field, it can be found that the leakage current of the ceramics with different compositions hardly changes under the action of external magnetic field. So it can be inferred that ceramics leakage current was not a major factor in the change in ceramics polarization.

### 3.4. Magnetic properties

The magnetization as a function of magnetic field ( $M$ - $H$  curves) of PTO/NFO ceramics is shown in Fig. 9. It is observed that the value of residual magnetization ( $M_r$ ) of all the ceramics increases with the increase of  $x$ , while the saturation magnetization ( $M_s$ ) of these samples decreases with the increase of  $x$ . Since the magnetization of the ceramic measured is a macroscopic property rather than a single particle, the phenomenon cannot be attributed to the uneven distribution of ferroelectric and ferromagnetic phases [9]. One reason for the above phenomenon may be the interface effect between the two phases. The decrease of the ferromagnetic phase will lead to the change of magnetic properties [28]. It may also be due to the polymerization and connection of two-phase materials, which may significantly affect the magnetic properties of the materials. The influencing factors of coercive magnetic field ( $H_c$ ) are mainly due to the grain size of magnetic materials. The  $H_c$  value

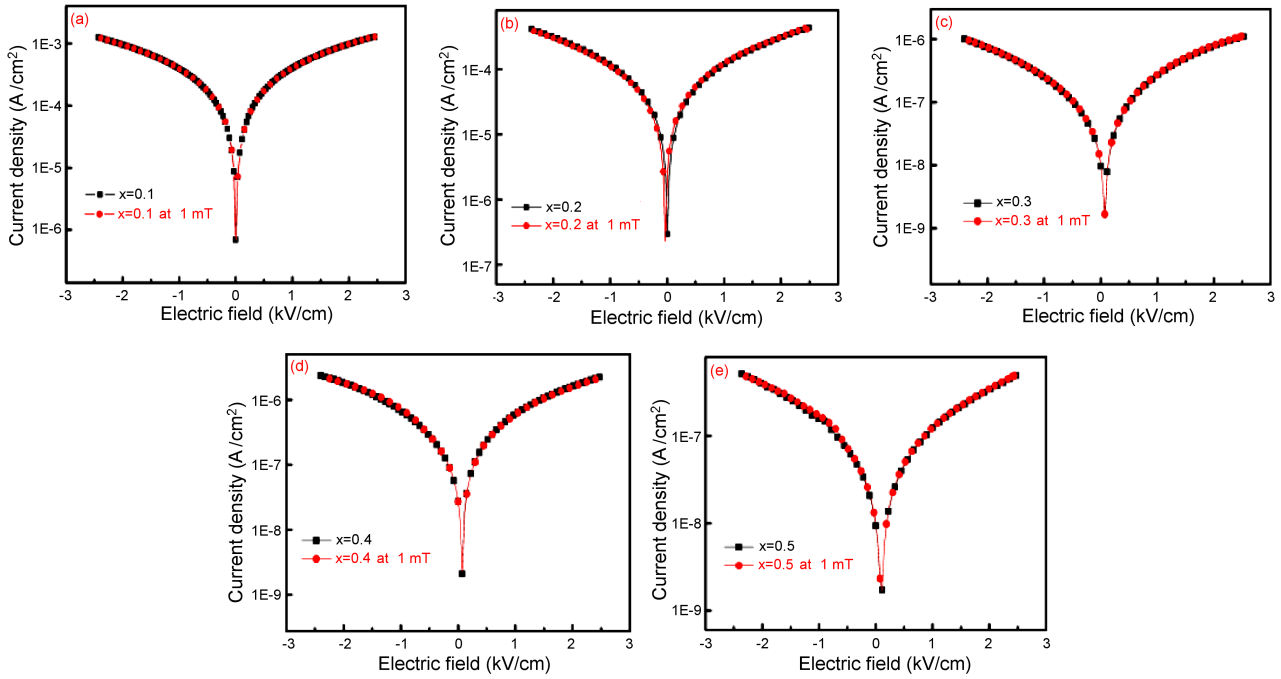


Figure 8. Leakage current and contrast diagram, measured under magnetic field, of  $x\text{PbTiO}_3/(1-x)\text{NiFe}_2\text{O}_4$ : a)  $x = 0.1$ , b)  $x = 0.2$ , c)  $x = 0.3$ , d)  $x = 0.4$  and e)  $x = 0.5$

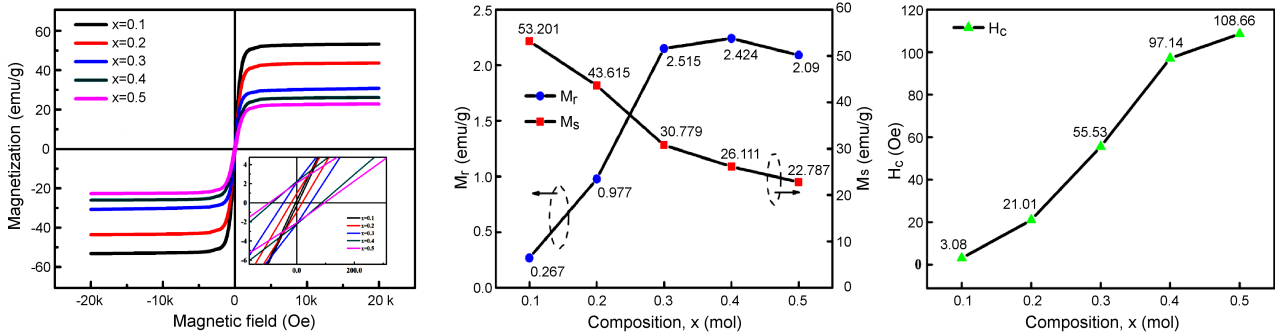


Figure 9. Magnetic properties of PTO/NFO ceramics

increases with the decrease of grain size, but when the grain size reaches a certain value,  $H_c$  decreases with the further decrease of grain size. The grain size of ceramics generally decreases with the increase of  $x$  (shown in Fig. 2), but the difference is not obvious, which needs further study. At the same time, magnetic anisotropy, impurity, defect and other reasons in the material may cause the change of coercivity.

#### IV. Conclusions

$x\text{PbTiO}_3/(1-x)\text{NiFe}_2\text{O}_4$  multiferroic materials were successfully prepared by mixing of sol-gel synthesized PTO and NFO powders, followed by their uniaxial pressing and sintering at  $1150^\circ\text{C}$ . The obtained ceramics have been proven to be PTO/NFO composite ceramics by XRD patterns. The surface and grain distribution are more uniform when  $x = 0.5$ , the ferroelectric performance, insulation performance and magnetoelectric coupling effect were also preferable among all the samples, while the magnetic properties of the

$0.4\text{PbTiO}_3/0.6\text{NiFe}_2\text{O}_4$  ceramics were the best due to the relative density structure and size effect. It was concluded that the leakage current of ceramics was not the main factor affecting the change of hysteresis loop of ceramics. However, since the principle of single variable is maintained, the electric field intensity added by ceramics in this paper was not high, so the next step was to improve the material compactness and other aspects, and study the corresponding situation in the case of high electric field.

**Acknowledgements:** The present work has been supported by the Chongqing Research Program of Basic Research and Frontier Technology (CSTC2018 jcyjAX0416, CSTC2019jcyj-msxmX0071), the Science and Technology Research Program of Chongqing Municipal Education Commission (KJZD-M201901501), the Scientific and Technological Research Young Program of Chongqing Municipal Education Commission (KJQN201801509, KJQN20190150), the Program for Creative Research Groups in University of Chongqing

(Grant No. CXQT19031), the Innovation Program for Chongqing's Overseas Returnees (cx2019159), the Excellent Talent Project in University of Chongqing (Grant No. 2017-35), the Science and Technology Innovation Project of Social Undertakings and Peoples Livelihood Guarantee of Chongqing (cstc2017shmsA90015), the Leading Talents of Scientific and Technological Innovation in Chongqing (CSTCCXLJRC201919), the Program for Technical and Scientific Innovation Led by Academician of Chongqing, the Latter Foundation Project of Chongqing University of Science & Technology (CKHQZZ2008002), and the Scientific & Technological Achievements Foundation Project of Chongqing University of Science & Technology (CKKJCG2016328), the Postgraduate technology innovation project of Chongqing University of Science & Technology (YKJCX1820205, YKJCX1820214, YKJCX1920203), the 9<sup>th</sup> Chongqing KeHui graduate student innovation and entrepreneurship competition (09111149, 09111260) and the student innovating projects of science of Chongqing (201811551014).

## References

- G. Chen, L. Cheng, H. Wu, S.L. Zhang, R.C. Xu, Q.W. Zhang, Z.D. Li, C.L. Fu, "Effect of mass ratio on the dielectric and multiferroic properties of  $\text{Co}_{0.5}\text{Zn}_{0.5}\text{FeCrO}_4/\text{Ba}_{0.85}\text{Ca}_{0.15}\text{Zr}_{0.1}\text{Ti}_{0.9}\text{O}_3$  composite ceramics", *Appl. Phys. A - Mater.*, **125** [12] (2019) 848.
- R.L. Gao, Q.M. Zhang, Z.Y. Xu, Z.H. Wang, W. Cai, G. Chen, X.L. Deng, X.L. Cao, X.D. Luo, C.L. Fu, "Strong magnetoelectric coupling effect in  $\text{BaTiO}_3@ \text{CoFe}_2\text{O}_4$  magnetoelectric multiferroic fluids", *Nanoscale*, **10** [26] (2018) 11750–11759.
- L. Bai, R.L. Gao, Q.M. Zhang, Z.Y. Xu, Z.H. Wang, C.L. Fu, G. Chen, X.L. Deng, W. Cai, "Influence of molar ratio on dielectric, ferroelectric and magnetic properties of  $\text{Co}_{0.5}\text{Mg}_{0.5}\text{Fe}_2\text{O}_4/\text{Ba}_{0.85}\text{Sr}_{0.15}\text{TiO}_3$  composite ceramics", *Process. Appl. Ceram.*, **13** [3] (2019) 257–268.
- R.L. Gao, Q.M. Zhang, Z.Y. Xu, Z.H. Wang, G. Chen, C.L. Fu, X.L. Deng, W. Cai, "Anomalous magnetoelectric coupling effect of  $\text{CoFe}_2\text{O}_4$ - $\text{BaTiO}_3$  binary mixed fluids", *ACS Appl. Electron. Mater.*, **1** [7] (2019) 1120–1132.
- R.C. Xu, S.L. Zhang, F.Q. Wang, Q.W. Zhang, Z.D. Li, Z.H. Wang, R.L. Gao, C.L. Fu, "The study of microstructure, dielectric and multiferroic properties of  $(1-x)\text{Co}_{0.8}\text{Cu}_{0.2}\text{Fe}_2\text{O}_4$ - $x\text{Ba}_{0.6}\text{Sr}_{0.4}\text{TiO}_3$  composites", *J. Electron. Mater.*, **48** [1] (2019) 386–400.
- R.L. Gao, L. Bai, Z.Y. Xu, Q.M. Zhang, Z.H. Wang, W. Cai, G. Chen, X.L. Deng, C.L. Fu, "Electric-field induced magnetization rotation in magnetoelectric multiferroic fluids", *Adv. Electron. Mater.*, **4** [6] (2018) 1800030.
- R.L. Gao, Q.M. Zhang, Z.Y. Xu, Z.H. Wang, C.L. Fu, G. Chen, X.L. Deng, X.D. Luo, Y. Qiu, W. Cai, "Enhanced multiferroic properties of  $\text{Co}_{0.5}\text{Ni}_{0.5}\text{Fe}_2\text{O}_4/\text{Ba}_{0.85}\text{Sr}_{0.15}\text{TiO}_3$  composites based on particle size effect", *J. Mater. Sci. Mater. Electron.*, **30** [11] (2019) 10256–10273.
- R.L. Gao, Z.H. Wang, G. Chen, X.L. Deng, W. Cai, C.L. Fu, "Influence of core size on the multiferroic properties of  $\text{CoFe}_2\text{O}_4@ \text{BaTiO}_3$  core shell structured composites", *Ceram. Int.*, **44** (2018) S84–S87.
- R.C. Xu, Z.H. Wang, R.L. Gao, S.L. Zhang, Q.W. Zhang, Z.D. Li, C.Y. Li, G. Chen, X.L. Deng, W. Cai, C.L. Fu, "Effect of molar ratio on the microstructure, dielectric and multiferroic properties of  $\text{Ni}_{0.5}\text{Zn}_{0.5}\text{Fe}_2\text{O}_4$ - $\text{Pb}_{0.8}\text{Zr}_{0.2}\text{TiO}_3$  nanocomposite", *J. Mater. Sci. Mater. Electron.*, **29** (2018) 16226–16237.
- R.L. Gao, X.F. Qin, Q.M. Zhang, Z.Y. Xu, Z.H. Wang, C.L. Fu, G. Chen, X.L. Deng, W. Cai, "Enhancement of magnetoelectric properties of  $(1-x)\text{Mn}_{0.5}\text{Zn}_{0.5}\text{Fe}_2\text{O}_4$ - $x\text{Ba}_{0.85}\text{Sr}_{0.15}\text{Ti}_{0.9}\text{Hf}_{0.1}\text{O}_3$  composite ceramics", *J. Alloys Compd.*, **795** (2019) 501–512.
- Z.X. Li, Z.H. Wang, R.L. Gao, W. Cai, G. Chen, X.L. Deng, C.L. Fu, "Dielectric, ferroelectric and magnetic properties of  $\text{Bi}_{0.78}\text{La}_{0.08}\text{Sm}_{0.14}\text{Fe}_{0.85}\text{Ti}_{0.15}\text{O}_3$  ceramics prepared at different sintering conditions", *Process. Appl. Ceram.*, **12** [4] (2018) 394–402.
- R.L. Gao, H. W. Yang, Y.S. Chen, J.R. Sun, Y.G. Zhao, B.G. Shen, "Ferroelectric polarization switching kinetics process in  $\text{Bi}_{0.9}\text{La}_{0.1}\text{FeO}_3$  films", *J. Appl. Phys.*, **114** (2013) 174101.
- R.L. Gao, Q.M. Zhang, Z.Y. Xu, Z.H. Wang, G. Chen, X.L. Deng, C.L. Fu, W. Cai, "A comparative study on the structural, dielectric and multiferroic properties of  $\text{Co}_{0.6}\text{Cu}_{0.3}\text{Zn}_{0.1}\text{Fe}_2\text{O}_4/\text{Ba}_{0.9}\text{Sr}_{0.1}\text{Zr}_{0.1}\text{Ti}_{0.9}\text{O}_3$  composite ceramics", *Compos. Part. B - Eng.*, **166** (2019) 204–212.
- X.F. Qin, R.C. Xu, H. Wu, R.L. Gao, Z.H. Wang, G. Chen, C.L. Fu, X.L. Deng, W. Cai, "A comparative study on the dielectric and multiferroic properties of  $\text{Co}_{0.5}\text{Zn}_{0.5}\text{Fe}_2\text{O}_4/\text{Ba}_{0.8}\text{Sr}_{0.2}\text{TiO}_3$  composite ceramics", *Process. Appl. Ceram.*, **13** [4] (2019) 349–359.
- R.L. Gao, X.F. Qin, T. Fan, R.C. Xu, H. Wu, Z.H. Wang, G. Chen, C.L. Fu, X.L. Deng, W. Cai, "Influence of  $\text{IrO}_2$  addition on magnetoelectric properties of  $\text{Ni}_{0.5}\text{Zn}_{0.5}\text{Fe}_2\text{O}_4/\text{Ba}_{0.8}\text{Sr}_{0.2}\text{TiO}_3$  composite ceramics", *J. Mater. Sci. Mater. Electron.*, **31** (2020) 2436–2445.
- Y.Z. Xue, R.C. Xu, Z.H. Wang, R.L. Gao, C.Y. Li, G. Chen, X.L. Deng, W. Cai, C.L. Fu, "Effect of magnetic phase on structural and multiferroic properties of  $\text{Ni}_{1-x}\text{Zn}_x\text{Fe}_2\text{O}_4/\text{BaTiO}_3$  composite ceramics", *J. Electron. Mater.*, **48** [8] (2019) 4806–4827.
- C.E. Ciomaga, M. Airimioaei, I. Turcan, A.V. Lukacs, S. Tascu, M. Grigoras, N. Lupu, J. Banyas, L. Mitoseriu, "Functional properties of percolative  $\text{CoFe}_2\text{O}_4$ - $\text{PbTiO}_3$  composite ceramics", *J. Alloys Compd.*, **775** (2019) 90–99.
- M. Meera Rawat, K.L. Yadav, "Structural, dielectric, ferroelectric and magnetic properties of  $(x)\text{CoFe}_2\text{O}_4$ - $(1-x)\text{BaTiO}_3$  composite", *IEEE. Trans. Dielectr. Electr. Insul.*, **22** [3] (2015) 1462–1469.
- S.B. Reddy, P.P. Singh, N. Raghu, "Effect of type of solvent and dispersant on NANO PZT powder dispersion for tape casting slurry", *J. Mater. Sci.*, **37** (2002) 929–934.
- X.F. Qin, H. Wu, R.C. Xu, R.L. Gao, Z.H. Wang, G. Chen, C.L. Fu, X.L. Deng, W. Cai, "Study on magnetoelectric properties of  $\text{Ni}_{0.5}\text{Zn}_{0.5}\text{Fe}_2\text{O}_4/\text{Ba}_{0.8}\text{Sr}_{0.2}\text{TiO}_3$  composite ceramics based on  $\text{Bi}_2\text{O}_3$  as combustion aid", *J. Mater. Sci. Mater. Electron.*, **31** (2020) 4073–4082.
- N.S. Negi, R. Kumar, H. Sharma, J. Shah, R.K. Kotnala, "Structural, multiferroic, dielectric and magnetoelectric properties of  $(1-x)\text{Ba}_{0.85}\text{Ca}_{0.15}\text{Ti}_{0.90}\text{Zr}_{0.10}\text{O}_3$ - $(x)\text{CoFe}_2\text{O}_4$  lead-free composites", *J. Magn. Magn. Mater.*, **456** (2018) 292–299.
- R.L. Gao, X.F. Qin, Q.M. Zhang, Z.Y. Xu, Z.H. Wang, C.L. Fu, G. Chen, X.L. Deng, W. Cai, "A

- comparative study of the dielectric, ferroelectric and anomalous magnetic properties of  $\text{Mn}_{0.5}\text{Mg}_{0.5}\text{Fe}_2\text{O}_4/\text{Ba}_{0.8}\text{Sr}_{0.2}\text{Ti}_{0.9}\text{Zr}_{0.1}\text{O}_3$  composite ceramics”, *Mater. Chem. Phys.*, **232** (2019) 428–437.
23. S.P. Ruan, J. Wang, L. Zhang, Y.G. Liu, J. Ma, L. Xuan, B.K. Xu, “Synthesis and dielectric properties of nanocrystalline  $\text{PbTiO}_3$ ”, *J. Funct. Mater. Dev.*, **9** [2] (2003) 139–142.
  24. C.Y. Li, R.C. Xu, R.L. Gao, Z.H. Wang, G. Chen, X.L. Deng, W. Cai, C.L. Fu, Q.T. Li, “A comparative study on the structural, dielectric, ferroelectric and magnetic properties of  $\text{CoFe}_2\text{O}_4/\text{PbZr}_{0.52}\text{Ti}_{0.48}\text{O}_3$  multiferroic composite with different molar ratios”, *J. Phys. Commun.*, **3** (2019) 125010.
  25. J.S. Kim, K.H. Lee, C.I. Cheon, “Crystal structure and the effect of annealing atmosphere on the dielectric properties of the spinels  $\text{MgAl}_2\text{O}_4$ ,  $\text{NiFe}_2\text{O}_4$ , and  $\text{NiAlFeO}_4$ ”, *J. Electroceram.*, **22** [1-3] (2009) 233–237.
  26. W. Cai, C. L. Fu, J. C. Gao, H. Q. Chen, “Effects of grain size on domain structure and ferroelectric properties of barium zirconate titanate ceramics”, *J. Alloys Compd.*, **480** [2] (2009) 870–873.
  27. W. Cai, J.C. Gao, C.L. Fu, L. Tang, “Dielectric properties, microstructure and diffuse transition of Ni-doped  $\text{Ba}(\text{Zr}_{0.2}\text{Ti}_{0.8})\text{O}_3$  ceramics”, *J. Alloys Compd.*, **487** [1-2] (2009) 668–674.
  28. R. Sharma, P. Pahuja, R.P. Tandon, “Structural, dielectric, ferromagnetic, ferroelectric and ac conductivity studies of the  $\text{BaTiO}_3\text{-CoFe}_{1.8}\text{Zn}_{0.2}\text{O}_4$  multiferroic particulate composites”, *Ceram. Int.*, **40** (2014) 9027–9036.